Rapid Reconfigurable OCDMA System Using Single-Phase Modulator for Time-Domain Spectral Phase Encoding/Decoding and DPSK Data Modulation

Zhensen Gao, *Student Member, IEEE*, Xu Wang, *Senior Member, IEEE*, Nobuyuki Kataoka, *Member, IEEE*, and Naoya Wada, *Member, IEEE*

***Abstract*—An optical-code-division-multiple-access (OCDMA) system with a novel modulation scheme for simultaneous generation of time-domain spectral phase encoding/decoding (SPE/SPD) and differential phase-shift keying (DPSK) data modulation that can be potentially rapidly reconfigured using only a single-phase modulator (PM) is proposed and experimentally demonstrated. The time-domain SPE is realized by stretching and compressing the ultrashort optical pulse through two-chirped fiber Bragg gratings with opposite dispersion and a high-speed PM for optical code (OC) generation and data modulation. The SPD has similar configuration as the SPE counterpart but using another PM synchronously driven by the complementary code pattern for OC recognition. Simulation investigation and experimental results both show that the code transition, dispersion mismatch between the encoding and decoding side, and the transmission fiber dispersion have detrimental effect on the en/decoding performance. In the experiment, 16-chip, 40-Gchip/s OC pattern and 2.5-Gb/s DPSK data modulation have been simultaneously generated using a single PM. The 2.5-Gb/s DPSK data have been successfully decoded and transmitted over 34 km fiber with $\mathrm{BER} < 10^{-9}$ for five OCs. The proposed scheme employs similar setup for transmitter and receiver, exhibiting the potential to simplify the architecture of the whole system, and improve the flexibility and confidentiality of OCDMA system.**

***Index Terms*—Fiber optics, optical-code-division-multiplexing (OCDM), phase modulation (PM), secure optical communication, spectral phase encoding/decoding (SPE/SPD).**

I. Introduction

DURING the past years, optical-code-division-multiple-access (OCDMA) has witnessed a large amount of research activities [1]–[3], mainly owning to its potential application in future broadband access network with unique features of high-speed all-optical processing, fully asynchronous transmission with low latency, simplified network management, flexible quality-of-service (QoS) control, and improved information security [4], [5]. In a typical OCDMA system, the optical pulse is encoded into a noise-like signal according to the unique optical code (OC) assigned to different users by the optical encoder at the transmitter, and multiple users can share the same transmission media, such as time and spectrum. At the receiver side, the optical decoder performs OC recognition by matched filtering, where the autocorrelation for the target OC produces a high-level output, while the cross correlation for undesired OC produces a low-level output [6], [7]. Finally, the original signal can be recovered after electrical processing.

Generally, the previous proposed OCDMA systems can be classified into two categories according to their working principles [8]: incoherent OCDMA adopting intensity-based code sequences and coherent OCDMA using phase-shifted optical sequences. The coherent OCDMA is more attractive for practical application because of its overall superior performance than the incoherent OCDMA and the development of compact and reliable en/decoding devices [5]. Proposed optical en/decoders include superstructured fiber Bragg grating [9], [10], planar lightwave circuit [11], [12], multiport en/decoder [13] for coherent time spreading (TS) OCDMA, and spatial lightwave modulator [14], [15], microring resonator [16], monolithically integrated en/decoders including array-waveguide-grating (AWG) and phase shifters [17] for coherent spectral phase encoding time spreading (SPECTS) OCDMA application. In SPECTS-OCDMA system, the spectral phase encoding (SPE) is realized by applying different phase shift onto different spectral component of an ultrashort optical pulse, which also results in time spreading of the short pulse as the coherent TS-OCDMA. Whereas the decoding is to give inverted phase changes to the corresponding spectral components by the proper decoder with a complementary phase shift pattern compared to that of the encoder. After the decoding, the phase of the resulting spectrum is frequency invariant, and therefore, the noisy pulse is temporally despread back to the original pulse shape. Previously, most of the SPECTS-OCDMA systems were realized in spectral domain, which makes the requirement of wavelength stability of the laser source very stringent.

Recently, we proposed a novel time-domain SPE scheme using two dispersive fibers with opposite dispersion and a high speed phase modulator (PM) for coherent OCDMA application

Manuscript received June 07, 2010; revised September 14, 2010, October 24, 2010; accepted November 09, 2010. Date of publication November 18, 2010; date of current version February 01, 2011. This work was supported in part by the Royal Society International Joint Project. The work of Z. Gao was supported by the International Travel Grant by the Royal Academy of Engineering.

Z. Gao and X. Wang are with the Joint Research Institute for Integrated Systems, School of Engineering and Physical Sciences, Heriot-Watt University, Edinburgh, EH14 4AS, U.K. (e-mail: x.wang@hw.ac.uk).

N. Kataoka and N. Wada are with the National Institute of Information and Communications Technology, Koganei, Tokyo 184-8795, Japan.

Color versions of one or more of the figures in this paper are available online at http://ieeexplore.ieee.org

Digital Object Identifier 10.1109/JLT.2010.2093558

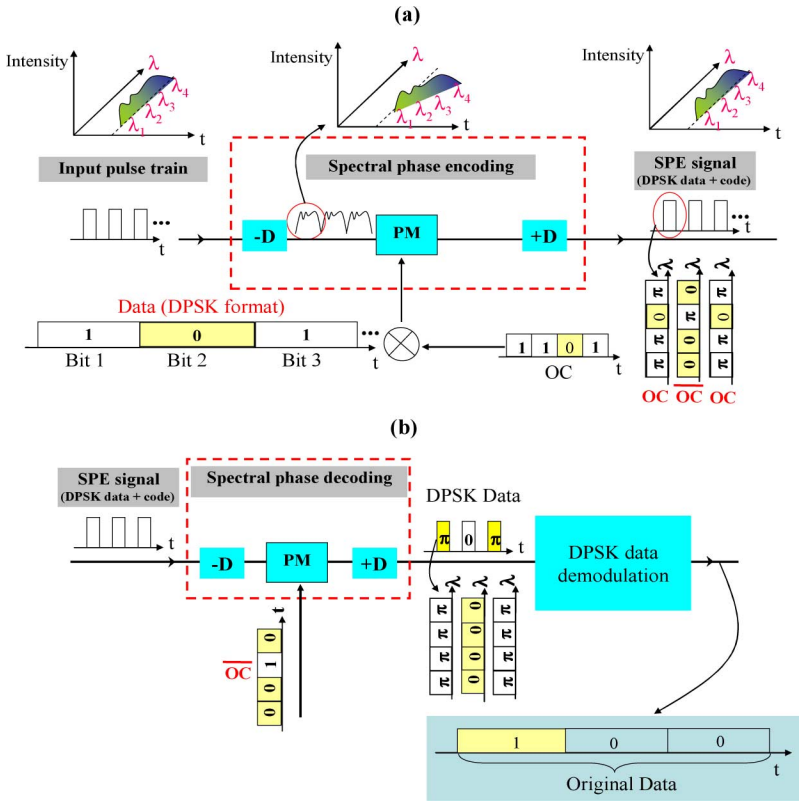

Fig. 1. Proposed scheme for: (a) SPE and DPSK data modulation using single PM and (b) SPD and DPSK data demodulation.

[18]. This scheme is very robust to the wavelength drift of the laser source, because every 1 GHz wavelength drift can be easily compensated by adjusting either the optical or electrical delay of $\sim$ 2.5 ps in the system. Unlike the conventional optical encoder/decoders that are either nonprogrammable or employing slow heater to configure the codes that cannot offer fast reconfigurable capability [17], the proposed scheme is very flexible in reconfiguring the OCs and compatible with the fiber optical system. Moreover, it exhibits the potential to combine the OC and differential phase-shift keying (DPSK) data by using only a single PM to improve the system flexibility, simplificity and reduce the cost. In our previous proof-of-principle experiments [19], [20], we have successfully demonstrated the feasibility of simultaneous generation of SPE with 8-chip, 20-Gchip/s OCs and DSPK data modulation using a single PM, and decoding using an AWG or a variable-bandwidth spectrum shaper-based spectral phase decoder. However, the accurate control of both the amplitude and phase in the spectral phase decoder is rather difficult that will greatly limit the code length and degrade the decoding as well as the transmission performance.

In this paper, we propose and experimentally demonstrate a novel OCDMA modulation scheme using only a single PM for simultaneous generation of either time-domain SPE/DSPK data modulation or time-domain spectral phase decoding (SPD), which can potentially provide rapid reconfigurability and improved security. In the proposed scheme, the time-domain SPD has similar configuration as the SPE counterpart but with another PM synchronously driven by the complementary code pattern for OC recognition. Linearly chirped fiber Bragg grating (LCFBG) is used in the time-domain SPE/SPD scheme with the advantages of good compactness, low insertion loss, ideal dispersion compensation, and serving as a dispersive component as well as an optical bandpass filter simultaneously. The proposed scheme has several potential advantages, with respect to the previous time-domain SPE system [18]–[20] that utilized a spectral phase decoder for spectral domain decoding: more flexible to rapidly reconfigure the OC and DPSK data with the potential to enhance the network security, potentially simplified network architecture by using similar setup for the transmitter and receiver, improved en/decoding performance and relaxed controlling accuracy of the amplitude/phase in the spectral phase decoder, all of which combine make our scheme more practical for OCDMA application and secure optical communication. The rest of the paper is organized as follows. In Section II , we present the principle of proposed SPE/SPD DPSK-OCDMA scheme using single PM; the experimental setup is described in Section III; in Section IV, we present the experimental results and discuss the decoding performance degradation due to the code transition, dispersion mismatch between the encoding and decoding side, and the transmission fiber dispersion. In the experiment, 2.5-Gb/s DPSK data have been successfully decoded and transmitted over 34 km fiber using the proposed time-domain SPE/SPD scheme with five 16-chip, 40-GHz/chip OC patterns. The conclusions are given in the last section.

II. Principle of Proposed SPE/SPD DPSK-OCDMA Scheme

Fig. 1 illustrates the operation principle of the proposed scheme. As shown in Fig. 1(a), the laser source gener-

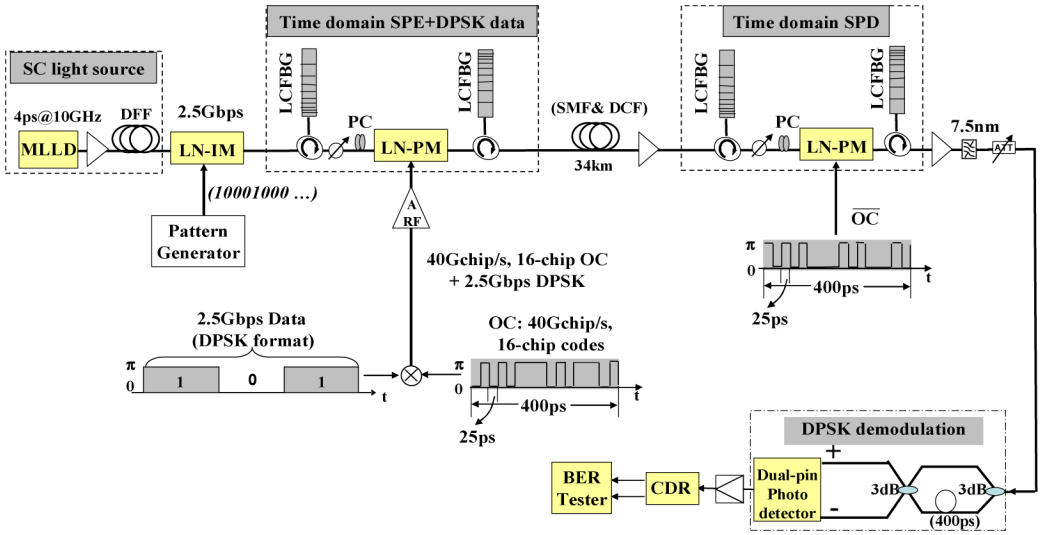

Fig. 2. Experimental setup of the proposed rapid reconfigurable time-domain SPE/SPD DPSK-OCDMA system.

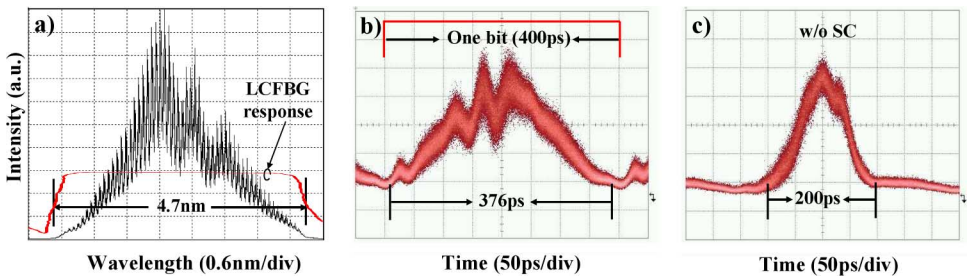

Fig. 3. (a) Spectrum after LCFBG; (b) waveform of stretched pulse with SC generation; (c) waveform of stretched pulse without SC generation.

ates an ultrashort optical pulse with a broadband spectrum $(\lambda_1, \lambda_2, \lambda_3, \lambda_4)$ for SPE. The SPE section is composed of a pair of dispersive devices with opposite dispersion values ($-$D and $+$D) and a high-speed PM. The first dispersive device with dispersion value of $-$D is used to stretch the pulse in time domain. Different spectral components of the input pulse will spread at different positions in one bit duration. The PM is driven by combining the DPSK data and OC patterns. The DPSK data are generated by precoding the original data (100. . .) into DPSK format (101. . .), and then mixed with the OC as follows to modulate the phase of the stretched optical signal: when the DPSK data are symbol "1," the PM is driven by OC (1101. . .), while if the symbol is "0," the PM is driven by $\overline{\text{OC}}$ (0010 . . .). Therefore, the SPE and DPSK data modulation can be achieved by using only a single PM (i.e., 1101, 0010, 1101. . .). After that, the second dispersive device with opposite dispersion value of +D is used to compress the stretched pulse in time domain and generate the DPSK data modulated SPE signal.

To recover the original data, the generated DPSK data modulated SPE signal has to be recognized by proper OC and then DPSK demodulated, as shown in Fig. 1(b). Time-domain SPD scheme, which has the similar configuration as the SPE that is composed of another pair of dispersive device and PM driven only by the complementary code pattern $\overline{\text{OC}}$ is used to perform the OC recognition. The spectral components of each bit are in phase after the decoding. For symbol "1," the total phase is "$\text{OC} + \overline{\text{OC}} = \pi$," while for symbol "0," the total phase is "$\overline{\text{OC}} + \overline{\text{OC}} = 0$." Therefore, the DPSK data are extracted from the SPE signal as (101. . .). The correctly decoded DPSK data can then be demodulated by a DPSK demodulator followed by a balanced detector to recover the original data (100 . . .). In the proposed scheme, the OC generation and DPSK data modulation are simultaneously generated by using single PM, while the OC recognition and DPSK data demodulation are achieved separately; therefore, the configuration of this system would be greatly simplified, and meanwhile, the flexibility and security can be significantly improved.

III. Experimental Setup

Fig. 2 shows the experimental setup of the proposed time-domain SPE/SPD scheme for simultaneous generation of SPE/SPD and DPSK data modulation. At the transmitter, a mode-locked-laser-diode (MLLD) produces nearly transform-limited $\sim$ 4 ps (FWHM) Gaussian-like pulses with a repetition rate of 10 GHz and 10-dB bandwidth of 2.5 nm, spectrally centered at 1550.28 nm. Supercontinuum (SC) generation based on the MLLD, an erbium-doped fiber amplifier (EDFA), and a piece of 2 km dispersion-flattened fiber (DFF) is employed to broaden the bandwidth of the original spectrum into $\sim$ 20 nm. A Mach–Zehnder intensity modulator (IM) driven by a pulse pattern generator (PPG) is used to convert the source repetition rate into 2.5 GHz. For the generation of time-domain SPE and DPSK data modulation, an LCFBG with

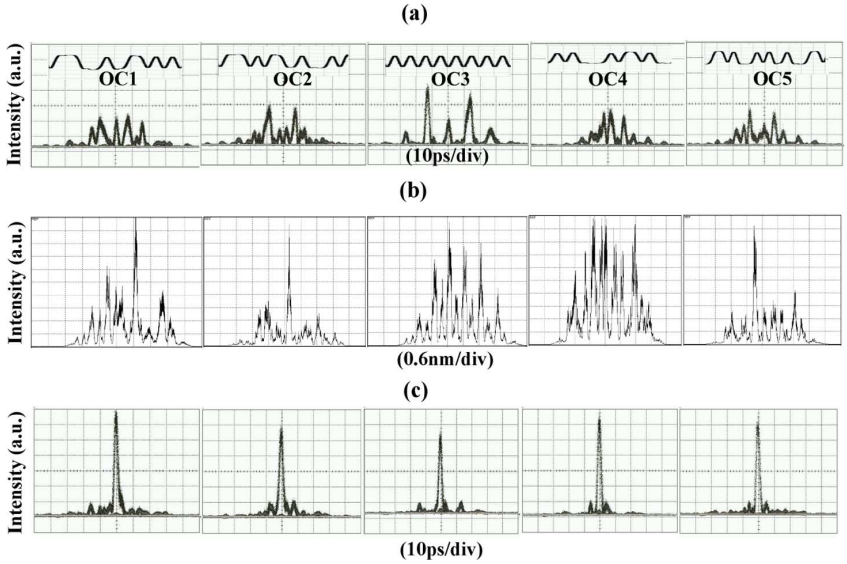

Fig. 4. (a) Encoded waveform (upper row), (b) encoded spectrum (middle row), and (c) autocorrelation signal for the five OCs.

10-dB bandwidth of $\sim$ 4.7 nm and dispersion slope of about -80 ps/nm is used to stretch the input optical pulse. Fig. 3(a) and (b) shows the spectrum and waveform of the stretched pulse after the LCFBG, respectively. Different spectral components spread into different positions in time domain because of the dispersion. As can be seen from Fig. 3(a), the tail of the input spectrum has been slightly cut into $\sim$ 4.7 nm due to the sharp spectral response of the LCFBG, which functions as a dispersive device as well as an optical bandpass filter. By using this LCFBG, the wavelength stability requirement is $\sim$ 0.5 nm for a bit-error-rate (BER) degradation from 10^{-9} to 10^{-2}. As shown in Fig. 3(b) , the stretched pulses exhibit similar profile as the input spectrum, covering about 376 ps within one bit period of 400 ps, and hence no obvious overlap between adjacent stretched pulses is observed in the experiment, which can significantly improve the decoding and transmission performance. Fig. 3(c) shows the waveform of the stretched pulse without SC generation, in which case the input spectrum is $\sim$ 2.5 nm and the stretched pulse occupies only $\sim$ 200 ps in time domain that will directly reduce the effective code length and degrade the peak power ratio (P/C) between the auto-/cross correlation signals. A PM driven by combining 16-chip 40-Gchip/s OC pattern (corresponding to 16-chip 40-GHz/chip spectral code pattern) and 2.5-Gb/s DPSK data then phase modulate the stretched optical pulse. The data rate mainly depends on the chip rate and code length in this system. For a chip rate of 40-Gchip/s and code length of no less than 16, the achievable maximum data rate is 2.5-Gb/s. To scale the data rate, one can either increase the chip rate, which is mainly limited by the electronic processing technology or decrease the code length and thus sacrifice the en/decoding performance. The DPSK data are mixed with the OC to drive the PM in such a way: when the DPSK data are symbol "1," the PM is driven by OC, while if symbol is "0," the PM is driven by $\overline{\mathrm{OC}}$. A tunable optical delay line is employed before the PM to accurately synchronize the OC pattern and stretched pulse, so the OC patterns can precisely modulate the phase of the corresponding spectral component. After that, another LCFBG with opposite dispersion of $+80$ ps/nm is used to compress the stretched pulse and generate the SPE signal. A span of 34 km single-mode fiber (SMF) is used as the transmission fiber in the experiment. Dispersion compensation fiber (DCF) module is employed to compensate the dispersion mismatch. Although we have previously demonstrated that the dispersion can be managed globally [18] because the dispersion before the encoding PM and after the decoding PM has been cancelled with each other, here, to show its flexibility of dispersion management, the dispersion is managed individually for each subsystem. To recover the original DPSK data, the generated SPE signal first has to be spectral phase decoded and then DPSK demodulated. The decoding part has the similar configuration as that of the encoding but the PM is driven only by the complementary code pattern $\overline{\mathrm{OC}}$. Note that careful temporal alignment between the encoding and decoding side by properly adjusting the tunable optical delay line before the PM is essential for decoding the SPE signal and improving the security, because it is quite difficult for the eavesdropper to recover the target data without proper synchronization even if he or she knows the applied OC. The correctly decoded signal is then directed into a 2.5-GHz DPSK demodulator followed by a balanced detector to recover the DPSK data. A 2.65-GHz low-pass filter is used after the balanced detector to perform data-rate detection. The BER is finally measured by an error detector.

IV. Results and Discussion

We have carried out an encoding/decoding experiment at first using five different 16-chips 40-Gchip/s OC patterns: two of them are from M-sequence, one is randomly selected and the other two are from Gold codes. The patterns used in the experiment are: OC1 (111000100110101) and OC2 (1110101100100010) are 15-chip M-sequence plus a zero, OC3 is (1010101010101010), OC4 (101000010110100), and OC5 (110100010100100) are 15-chip Gold code plus a zero. Fig. 4 shows the encoded waveform (upper trace), encoded

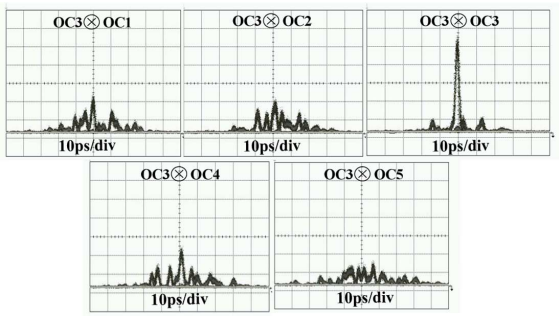

Fig. 5. Waveforms of the cross-correlation signals for OC3 with the other codes.

spectrum (middle trace), and autocorrelation (lower trace) measured by a 10 GHz optical sampling oscilloscope for the five codes after transmission. All the five codes have been successfully decoded in the experiment. The cross-correlation signals for OC3 are also shown in Fig. 5, from which one can see that the P/C between the auto/cross correlations has been improved to ~ 3 (compared to that of no SC generation with a maximum of P/C ~ 2 because of the relatively short effective code length of $\sim$ 8). To further improve the P/C, the peak intensity of the autocorrelation signal has to be increased. It is worth noting from the lower trace in Fig. 4 that there are some low sidelobes in the decoded waveforms, which can be partially ascribed to the nonideal synchronization between the encoding and decoding side as well as the modulation index difference between the two PMs. In addition, there are several other factors that need to be taken into account: code transition of the electrical signal from the PPG, dispersion mismatch of the LCFBGs between the encoding and decoding side, and the residual dispersion of the transmission fiber SMF and DCF.

Fig. 6 depicts the effect of code transition, which is defined as $\eta = a/b$ in the inset of Fig. 6(b) on the encoding/decoding performance for OC3. As can be seen from Fig. 6(a), the code transition will induce more pedestal pulses in the encoded waveform compared to the simulated encoded waveform in Fig. 6(b) that without code transition. The dashed blue line in Fig. 6(a) is the simulated encoded waveform with code transition of 45%, which agrees well with the experimental result (solid line). In the experiment, as the SPD configuration is similar to the encoding part, the relative code transition between the two PPGs in the encoding and decoding side will significantly affect the decoding performance. Fig. 6(c) shows the decoded waveform with identical code transition between the encoding and decoding, from which one can see that the decoded waveform still exhibit well-defined autocorrelation peak pulse while for different code transition, too many sidelobes in the decoded waveform appears, as can be seen from the inset in Fig. 6(d). The peak-to-wing ratio (P/W) and peak intensity versus the relative code transition are also shown in Fig. 6(d), respectively. As the relative code transition increases, both the P/W and peak intensity gradually decrease that will significantly degrade the transmission performance. However, even if the absolute code transition in each PPG is very large, there is no obvious degradation of the decoding performance when the relative code transition between the two PPGs is approximately zero.

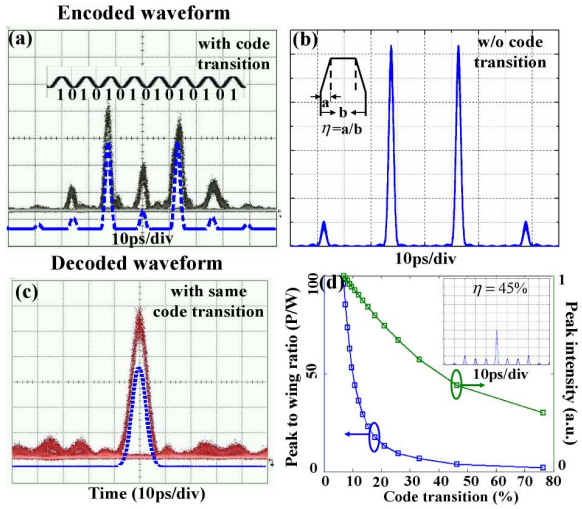

Fig. 6. (a) Encoded waveform (solid line) and simulated waveform (dashed line) with code transition; (b) encoded waveform without code transition; (c) decoded waveform (solid line) and simulated waveform (dashed line) with identical code transition in the encoding and decoding side; (d) P/W and peak intensity versus relative code transition. Inset: is the decoded waveform for $\eta = 45\%$.

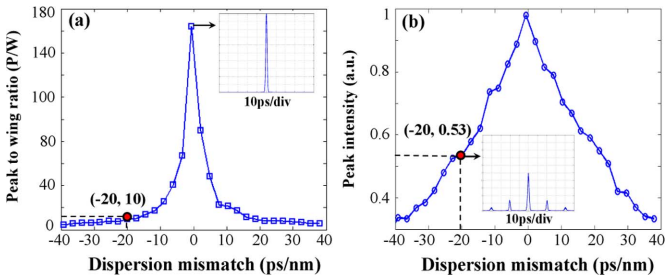

Fig. 7. (a) P/W and (b) peak intensity of the decoded waveform versus the dispersion mismatch. Insets: are the simulated decoded waveforms.

Besides the code transition, the dispersion mismatch in the encoding and decoding side is another key factor for the decoding performance. Assuming the dispersion has been fully compensated in both the encoding ($-$D1, D1) and decoding side ($-$D2, D2), but there is dispersion mismatch between them (D1 $\neq$ D2). Fig. 7(a) and (b) shows the P/W and peak intensity of the decoded waveform versus the dispersion mismatch for OC3, respectively. As the dispersion mismatch increases, the peak intensity gradually decreases and the sidelobes are generated in the decoded waveform, and hence the P/W dramatically decreases. The tolerance of dispersion mismatch is calculated to be $\sim \pm 20$ ps/nm for a minimum P/W and peak of 10 and 0.53, which is a little strict for practical application. To address this issue, we utilize two pairs of LCFBGs with identical dispersion in the encoding and decoding side instead of a dispersion fiber, so the effect of dispersion mismatch is easily eliminated in the experiment.

In addition, since the proposed SPE/SPD scheme is performed in time domain, the residual dispersion of the SMF and DCF cannot be neglected. Fig. 8(a) shows the measured and simulated decoded waveform considering the residual dispersion of 20 ps/nm in the transmission fiber for OC1, from which one can see that the asymmetric sidelobes of the simulated

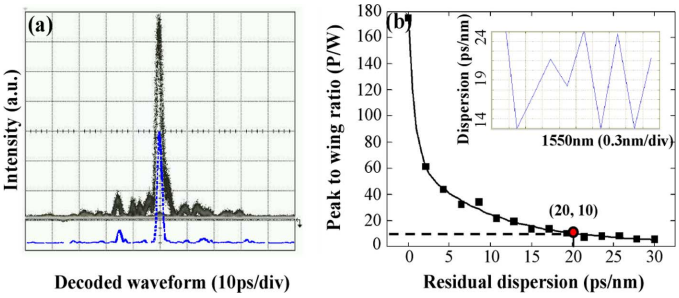

Fig. 8. (a) Measured (solid gray line) and simulated (dashed blue line) decoded waveform with residual dispersion of $\sim$ 20 ps/nm for OC1; (b) P/W versus residual dispersion of the transmission fiber. Inset: is the measured dispersion of the transmission fiber.

decoded waveform agree well with the experimental result, which verifies the decoding performance degradation due to the residual dispersion in the SMF and DCF. The P/W versus the residual dispersion is depicted in Fig. 8(b), from which one can see that the P/W is very sensitive to the residual dispersion and it will dramatically decreases with the increase of the residual dispersion. The inset in Fig. 8(b) is the measured total dispersion of the SMF and DCF in the experiment. Although the dispersion compensation is not ideal in the experiment with a residual dispersion of around 20 ps/nm at 1550.28 nm, corresponding to a P/W of ~ 10 , it is enough for the SPE/SPD DPSK-OCDMA system.

Finally, we have carried out a proof-of-principle experiment with the proposed setup for simultaneous generation of SPE and DPSK data modulation using single PM, and a 2.5-Gb/s DPSK data transmission experiment using the time-domain SPD scheme with 16-chip 25-ps/chip OC patterns. A trial of fixed data pattern 010100111001 for OC1 has been done at first, as shown in Fig. 9. The original data (a) is first precoded into DPSK data format (b) 011000101110 and then mixed with the OC1 to drive the PM in the encoding part, whose electrical waveform is shown in Fig. 9(c). The combined DPSK data and OC1 look like a pseudorandom bit sequence (PRBS) that is not easy to directly extract the DPSK data. Fig. 9(d) shows the waveform of the encoded SPE signal, which is indistinguishable for symbol "0" and "1." In the receiver side, the complementary code $\overline{\text{OC1}}$ is used to drive the second PM to generate the decoded signal as shown in Fig. 9(e), from which one can see the decoded signal for symbol "0" and "1" have similar waveform but totally different phase according to the DPSK data ($0\pi\pi000\pi0\pi\pi\pi0\ldots$). Fig. 9(f) shows the recovered data pattern after the DPSK demodulator and balanced detector which is exactly the original data pattern: 010100111001, indicating the feasibility of the proposed time domain SPE/SPD DPSK scheme. In addition, the 2.5-Gb/s DPSK data transmission experiment has been carried out using $2^7 - 1$ PRBS for all the five codes. The measured BER for back-to-back (B-to-B) and transmission with the five codes are shown in Fig. 10(a) and (b), respectively. Error-free ($\text{BER} < 10^{-9}$) has been achieved in both cases for all the codes though the optical received power is a little high due to the lack of a 2.5 GHz clock and data recovery circuit at the time of this experiment. The power penalty for the transmission is less than 1 dB. Clear eye opening have been achieved for all the

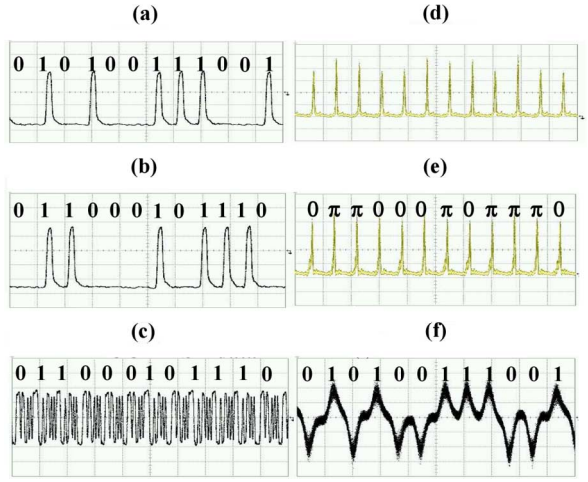

Fig. 9. Fixed data pattern trial: (a) original data pattern: 010100111001; (b) precoded DPSK data: 011000101110; (c) combined OC3 and DPSK data; (d) waveform of generated SPE signal; (e) waveform of decoded signal; and (f) recovered data pattern: 010100111001.

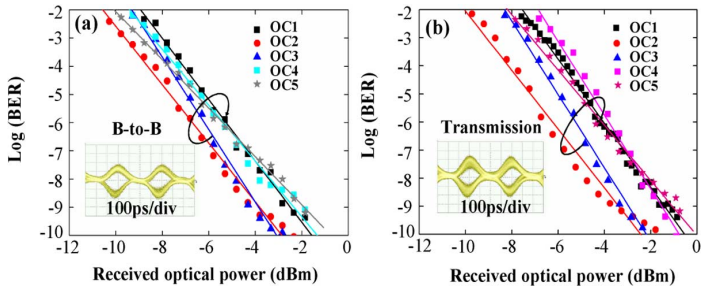

Fig. 10. BER performance for (a) back-to-back and (b) transmission over 34 km SMF and DCF.

five codes which demonstrate the proposed SPE/SPD scheme using single PM for OC generation and DPSK data modulation, and decoding using time-domain SPD scheme. Based on this scheme, the OC can even be rapidly bit-by-bit reconfigured and scrambled with the DPSK data to significantly enhance the data confidentiality for secure optical communication. In a multiuser environment, the multiple-access-interference (MAI) existing in any OCDMA system may impair the performance of the target user since the code length and P/C is not very high in this system. By using optical time gating technique [21] to reduce the effect of MAI, it is possible to support other active interfering users to improve both the capacity and security.

V. Conclusion

We have proposed and experimentally demonstrated an OCDMA modulation scheme using only a single PM for simultaneous generating and decoding of time-domain spectral phase encoded signal and DPSK data modulation. In the experiment, five 16-chip 40-GHz/chip OC patterns and 2.5-Gb/s DPSK data modulation have been generated using single PM. Transmission of the 2.5-Gb/s DPSK data over 34 km fiber with $\text{BER} < 10^{-9}$ has been demonstrated successfully. The proposed scheme has simple configuration and enables rapid reconfiguring the OC, exhibiting the potential to improve the flexibility and enhance the system security.

ACKNOWLEDGMENT

The authors would like to thank H. Sumimoto of the National Institute of Information and Communications Technology for his technical support in the experiment. They would also like to thank the anonymous reviewers for their valuable comments to enhance the quality of this paper.

REFERENCES

[1] P. R. Prucnal, M. A. Santoro, and T. R. Fan, "Spread spectrum fiber-optic local area network using optical processing," *J. Lightw. Technol.*, vol. 4, no. 5, pp. 547–554, May 1986.

[2] D. D. Sampson, G. J. Pendock, and R. A. Griffin, "Photonic code-division multiple-access communications," *Fiber Integr. Opt.*, vol. 16, pp. 126–157, 1997.

[3] J. A. Salehi, A. M. Weiner, and J. P. Heritage, "Coherent ultrashort light pulse code-division multiple access communication systems," *J. Lightw. Technol.*, vol. 8, no. 3, pp. 478–491, Mar. 1990.

[4] A. Stock and E. H. Sargent, "The role of optical CDMA in access networks," *IEEE Commun. Mag.*, vol. 40, no. 9, pp. 83–87, Sep. 2002.

[5] X. Wang and K. Kitayama, "Analysis of beat noise in coherent and incoherent time-spreading OCDMA," *J. Lightw Technol.*, vol. 22, no. 10, pp. 2226–2235, Oct. 2004.

[6] Z. Jiang *et al.*, "Four-user, 2.5-Gb/s, spectrally coded OCDMA system demonstration using low-power nonlinear processing ," *J. Lightw. Technol.*, vol. 23, no. 1, pp. 143–158, Jan. 2005.

[7] X. Wang, N. Wada, T. Miyazaki, G. Cincotti, and K. Kitayama, "Field trial of 3-WDM × 10-OCDMA × 10.71-Gb/s asynchronous WDM/DPSK-OCDMA using hybrid E/D without FEC and optical thresholding," *J. Lightw. Technol.*, vol. 25, no. 1, pp. 207–215, Jan. 2007.

[8] K. I. Kitayama, "Code division multiplexing lightwave networks based upon optical code conversion," *IEEE J. Sel. Areas Commun.*, vol. 16, no. 7, pp. 1209–1319, Sep. 1998.

[9] P. C. Teh, P. Petropoulos, M. Ibsen, and D. J. Richardson, "A comparative study of the performance of seven- and 63-chip optical code-division multiple-access encoders and decoders based on superstructured fiber Bragg gratings," *J. Lightw. Technol.*, vol. 9, no. 9, pp. 1352–1365, Sep. 2001.

[10] X. Wang, K. Matsushima, A. Nishiki, N. Wada, and K. Kitayama, "High reflectivity superstructured FBG for coherent optical code generation and recognition ," *Opt. Exp.*, vol. 12, pp. 5457–5468, 2004.

[11] R. G. Broeke, J. Cao, C. Ji, S. W. Seo, Y. Du, N. K. Fontaine, J. H. Baek, J. Yan, F. M. Soares, F. Olsson, S. Lourdudoss, A. H. Pham, M. Shearn, A. Scherer, and S. J. Ben Yoo, "Optical-CDMA in InP," *IEEE J. Sel. Top. Quantum Electron.*, vol. 13, no. 5, pp. 1497–1507, Sep. 2007.

[12] B. Huiszoon *et al.*, "Integrated parallel spectral OCDMA en/decoder," *IEEE Photon. Technol. Lett.*, vol. 19, no. 7, pp. 528–530, Apr. 2007.

[13] G. Cincotti, N. Wada, and K. Kitayama, "Characterization of a full encoder/decoder in the AWG configuration for code-based photonic routers—Part I: Modeling and design," *J. Lightw. Technol.*, vol. 24, no. 1, pp. 103–112, Jan. 2006.

[14] Z. Jiang, D. Seo, S. Yang, D. E. Leaird, R. V. Roussev, C. Langrock, M. M. Fejer, and A. M. Weiner, "Four-user 10-Gb/s spectrally phase-coded O-CDMA system operating at ∼ 30 fJ/bit," *IEEE Photon. Technol. Lett.*, vol. 17, no. 3, pp. 705–707, Mar. 2005.

[15] R. P. Scott, W. Cong, K. Li, V. J. Hernandez, B. H. Kolner, J. P. Heritage, and S. J. Ben Yoo, "Demonstration of an error-free 4 × 10 Gb/s multiuser SPECTS O-CDMA network testbed," *IEEE Photon. Technol. Lett.*, vol. 16, no. 9, pp. 2186–2188, Sep. 2004.

[16] A. Agarwal, P. Toliver, R. Menendez, T. Banwell, J. Jackel, and S. Etemad, "Spectrally efficient six-user coherent OCDMA system using reconfigurable integrated ring resonator circuits," *IEEE Photon. Technol. Lett.*, vol. 18, no. 18, pp. 1952–1954, Sep. 2006.

[17] J. Cao *et al.*, "Demonstration of spectral phase O-CDMA encoding and decoding in monolithically integrated arrayed-waveguide-grating-based encoder," *IEEE Photon. Technol. Lett.*, vol. 18, no. 24, pp. 2602–2604, Dec. 2006.

[18] X. Wang and N. Wada, "Spectral phase encoding of ultra-short optical pulse in time domain for OCDMA application ," *Opt. Exp.*, vol. 15, no. 12, pp. 7319–7326, Jun. 2007.

[19] Z. Gao, X. Wang, N. Kataoka, and N. Wada, "Demonstration of time domain spectral phase encoding/DPSK data modulation using single phase modulator," in *IEEE LEOS Summer Topical 2009*, New port, CA, USA, 2009, pp. 21–22, Paper TuA3.1.

[20] X. Wang, Z. Gao, N. Kataoka, and N. Wada, "Time domain spectral phase encoding/DPSK data modulation using single phase modulator for OCDMA application," *Opt. Exp.*, vol. 18, no. 10, pp. 9879–9890, 2010.

[21] P. Petropoulos, N. Wada, P. C. Teh, M. Ibsen, W. Chujo, K. Kitayama, and D. J. Richardson, "Demonstration of a 64-chip OCDMA system using superstructured fibre Bragg gratings and time gating-detection," *IEEE Photon. Technol. Lett.*, vol. 13, no. 11, pp. 1239–1241, Nov. 2001.

Zhensen Gao (S'10) received the B.S. and M.S. degrees from the Department of Physics, Harbin Institute of Technology, Harbin, China, in 2006 and 2008, respectively. He is currently working toward the Ph.D. degree in the Department of Electrical Engineering, Heriot-Watt University, Edinburgh, U.K.

Xu Wang (S'91–M'98–SM'06) received the B.S. degree in physics from Zhejiang University, Hangzhou, China, in 1989, the M.S. degree in electronics engineering from the University of Electronics Science and Technology of China (UESTC), Chengdu, China, in 1992, and the Ph.D. degree in electronics engineering from the Chinese University of Hong Kong (CUHK), in 2001.

From 1992 to 1997, he was a Lecturer at the National Key Laboratory of Fiber Optic Broadband Transmission and Communication Networks, UESTC. During 2001–2002, he was a Postdoctoral Research Fellow at the Department of Electronic Engineering, CUHK. From 2002 to 2004, he was at the Department of Electronic and Information Systems, Osaka University, Osaka, Japan, as a Telecommunications Advancement Organisation (TAO) Research Fellow. From 2004 to 2007, he was an Expert Researcher in the National Institute of Information and Communications Technology, Tokyo, Japan. He joined the School of Engineering and Physical Sciences, Heriot-Watt University, Edinburgh, U.K., as a Senior Lecturer in July 2007. He is the author or coauthor of more than 110 published technical papers and the first author of more than 80 among them. He has filed five patents and delivered over 30 invited talks in international conferences. His current research interests include fiber-optic networks, optical code-division multiplexing, optical packet switching, microwave photonics, and optic signal processing.

Dr. Wang was awarded the Telecommunications Advancement Research Fellowship by the TAO of Japan in 2002 and 2003.

Nobuyuki Kataoka (S'03–M'06) received the B.E., M.E., and Dr. Eng. degrees from Osaka University, Osaka, Japan, in 2001, 2003, and 2006, respectively.

In 2006, he joined the National Institute of Information and Communications Technology, Tokyo, Japan. His current research interests include photonic networks, such as optical packet switching, optical add/drop multiplexing, and optical code division multiple access.

Dr. Kataoka is a member of the Institute of Electronics, Information and Communication Engineers of Japan.

Naoya Wada (M'97) received the B.E., M.E., and Dr. Eng. degrees in electronics from Hokkaido University, Sapporo, Japan, in 1991, 1993, and 1996, respectively.

In 1996, he joined the Communications Research Laboratory, Ministry of Posts and Telecommunications, Tokyo, Japan. He is currently a Project Leader and Research Manager of the Photonic Network Group, National Institute of Information and Communications Technology, Tokyo, Japan. He is the author or coauthor of more than 70 papers published in refereed journals and more than 200 papers published in refereed international conferences. His research interests include photonic networks and optical communication technologies, such as optical packet switching network and optical code-division multiple access system.

Dr. Wada is a member of the IEEE Comsoc, the IEEE Lasers and Electro-Optics Society, the Institute of Electronics, Information and Communication Engineers (IEICE), the Japan Society of Applied Physics, and the Optical Society of Japan. He was the recipient of the 1999 Young Engineer Award from the IEICE of Japan, and the 2005 Young Researcher Award from the Ministry of Education, Culture, Sports, Science, and Technology.